Supporting information

Chemical structural characteristics of HULIS and other fractionated organic matter in urban aerosols: Results from mass spectral and FT-IR analysis

*Qingcai Chen[1], Fumikazu Ikemori[1,2], Hayato Higo[3], Daichi Asakawa[4], and Michihiro Mochida[*1]*

[1]Graduate School of Environmental Studies, Nagoya University, Nagoya, Japan

[2]Nagoya City Institute for Environmental Sciences, Nagoya, Japan

[3]Fukuoka City HAKATA Health & Welfare Center, Fukuoka, Japan

[4]Osaka City Institute of Public Health and Environmental Sciences, Osaka, Japan

*Corresponding author: mochida.michihiro@g.mbox.nagoya-u.ac.jp

Contents:

Tables: 8

Figures: 7

References: 24

S1. Acronym definitions

WSOM: water-soluble organic matter

WISOM: water insoluble organic matter

HULIS-n: humic-like substances with neutral nature in water-soluble organic matter

HULIS-a: humic-like substances with acidic nature in water-soluble organic matter

HP-WSOM: high-polarity water-soluble organic matter

EOM: extracted organic matter

EOC: extracted organic carbon

S2. Assessment of extraction with water

The separation of WSOM from WISOM is assessed according to the method in Psichoudaki and Pandis.[1] The fraction (f_A) of organic compound A in the aqueous phase after the extraction procedure depends on the solubility of A in water:

$$f_A = \frac{S_A P}{S_A P + \alpha C_{OA}(1 - f_{WSOM})} \tag{1}$$

where S_A is the solubility of organic compound A (g L^{-1}), P is the volume ratio of water to sampled air (cm^3 m^{-3}), α is the ratio of the molecular weight of WSOM to that of TOM, f_{WSOM} is the mass ratio of WSOM to TOM, and C_{OA} is the mass concentration of TOM in the atmosphere (μg m^{-3}). If a water extraction is carried out sequentially n times, the fraction of A in WSOM (f_A') is given by:

$$f_A{}' = 1 - (1 - f_A)^n \tag{2}$$

In this study, single-time extraction with $P \approx 0.2$ cm^3 m^{-3} was applied to the measurement of WSOC using TOC-V/CPH, whereas three sequential extractions were applied to the measurements using HR-AMS, FT-IR, and soft-ionization MS. We obtained f_A and $f_A{}'$ as a function of solubility (Figure S5) using the following assumptions: (1) EOM is the sum of WSOM and WISOM and (2) α is calculated from M_n of WSOM (mean: 220 Da) and EOM (mean: 330 Da), which were estimated from soft-ionization mass spectrometry (Table 1).

Figure S5 presents the fraction of organics in WSOM as a function of solubility. Although a condition with low P (≈ 0.02 cm^3 m^{-3}) was applied to the extraction of WSOM (cyan curve), three consecutive extractions led to a higher fraction (blue curve), which is comparable to that of single extraction with $P = 0.1$ cm^3 m^{-3} (pink curve), a value recommended by Psichoudaki and Pandis.[1] The efficiency of single time extraction with $P = 0.2$ cm^3 m^{-3} for the analysis of WSOC was also close to this recommended condition. This result indicates that the WSOM extracted by the two methods (single-time extraction with $P \approx 0.2$ cm^3 m^{-3} and three sequential extractions with $P \approx 0.02$ cm^3 m^{-3}) were similar. This finding is in line with the result that the concentrations of WSOC derived from the TOC-analyzer (mean ± SD: 1.64 ± 0.49 μg m^{-3}, $P \approx 0.2$ cm^3 m^{-3}) and those from the HR-AMS (1.70 ± 0.56 μg m^{-3}, $P \approx 0.02$ cm^3 m^{-3}) were very similar.

S3. Solvent extraction and off-line HR-AMS analysis of organics

To evaluate the recovery of organics from TSP samples throughout the solvent extraction

procedure, we compared the concentrations of extracted OC (WISOC + WSOC) derived from the analysis using HR-AMS and those of TOC derived from the TOC analyzer (Figure S6). The recoveries of OC were calculated to be $92 \pm 5.3\%$ (mean $\pm$ SD; $n = 12$; $r^2 = 0.93$) and $102 \pm 11\%$ (mean $\pm$ SD; $n = 12$; $r^2 = 0.84$) with the application of thermal/optical transmittance (TOT) and reflectance (TOR) methods, respectively, for the analysis using the TOC analyzer. The results suggest that nearly all organics were extracted from the TSP samples. This high recovery may be due to the sequential extraction process using multiple solvents of different polarities. The result in Figure S6 also shows that the concentrations of WSOC from different analytical approaches (AMS and TOC-VCPH) and different extraction conditions (once and three times) agree well ($n = 12$; $r^2 = 0.92$). The concentrations of WSOC from the HR-AMS correspond to $105 \pm 19\%$ (mean $\pm$ SD; $n = 12$) of those from TOC-VCPH.

Note that the adsorption of gaseous semi-volatile organic compounds onto the quartz filters leads to positive artifacts in the organic carbon levels, and that the volatilization of semi-volatile organic compounds in collected particles to the passing airstream leads to negative artifacts. The potential sampling artifacts were often dominated by OC adsorption and have been reported in the range of +20% to +55% for different sampling sites.[2-5] However, there is no simple way to correct for sampling artifacts.[6] Here, we roughly estimate this positive artifact as follows. Whereas gaseous organic compounds that adsorbed on quartz filters can be detected using carbon analyzer, those volatile organic compounds may not be detected using HR-AMS because of their vaporization in the diffusion scrubbers (one with silica gel and the other with activated carbon mixed with 12 wt% silica gel). If adsorbed organics on filters fully evaporated in the

scrubbers, the gas adsorption artifacts on quartz filters are calculated to be only 8% by the difference in TOC determined from the carbon analyzer (based on the TOT method) and that from HR-AMS. Therefore, a substantial positive artifact is not evident.

The reproducibility of the quantification of WISOM, WSOM, HULIS-n, HULIS-a and HP-WSOM was assessed by the extraction and the HR-AMS analysis of an identical aerosol sample (an extra filter sample) three times; the relative standard deviation (RSD) of the concentrations of WISOM, WSOM, HULIS-n, HULIS-a and HP-WSOM were 10.8%, 2.8%, 0.6%, 0.5%, and 5.8%, respectively. The blank levels were also assessed with HR-AMS analysis for a blank filter three times; they corresponded to 1.7%, 0.6%, 4.4%, 3.8%, and 1.6% of the lowest concentrations of the solutions of WISOM, WSOM, HULIS-n, HULIS-a and HP-WSOM for the HR-AMS analysis, respectively. The low RSD and low blank levels suggest that the process for quantifying organics, including aerosol sampling, solvent extraction, separation using SPE, and off-line HR-AMS analysis, was reliable. The reproducibility of the ion group and the elemental analyses for the off-line HR-AMS analysis of organics was also examined; the RSD of the relative intensities of six ion groups (CH, CO, CHO_1, $CHO_{>1}$, CHON, and CS) and the elemental ratios (H/C, O/C, and N/C) were, respectively, in the ranges of 0.5% to 17.5% and 0.2% to 10.1% for WISOM, WSOM, HULIS-n, HULIS-a and HP-WSOM (n = 3 for respective fractions).

S4. Fractionation of organics using SPE

The HLB column, which was used to separate low-polarity water soluble organics from the water extracts of atmospheric aerosols,[7, 8] was used for the fractionation of WSOM. The HLB column contains hydrophile-lipophile balanced material (N-vinyl pyrrolidone and divinyl benzene polymeride); the advantages are that irreversible adsorption is insignificant and that they are resistant to drying. Based on the adsorption mechanism of HLB, organics with different polarities in WSOM can be fractionated. Three fractions were isolated from WSOM using Oasis HLB in a manner analogous to that described in Varga et al. and Lin et al. as follows:[7, 8]

1) First, the pH of the water extract was adjusted to 7 with 0.01 M NaOH (Sigma-Aldrich, ≥99.99) solution, and it was then passed through the HLB column (200 mg, pre-activated by 6 mL MeOH and 6 ml Fluka water), followed by the addition of 2×0.5 ml of Fluka water to wash residual ions/species that were not retained. The HLB column was dried under a N_2 flow by Visiprep DL vacuum manifold (Supelco). Then, adsorbed species were eluted by 2 mL of methanol containing 2 wt% ammonia. The extract was fully dried under a nitrogen flow and redissolved with 6 g of MeOH. This organic fraction is referred to as humic-like substances with a neutral nature in WSOM (HULIS-n), because they favor adsorption on the column, which suggests small abundance of polar carboxylic groups.

2) Second, the effluent in the first step was collected in a 15-mL pre-cleaned sample bottle, and its pH was adjusted to 2 with 1 M HCl solution (Fluka, for trace analysis). The effluent was then passed through the HLB column, followed by the addition the 2×0.5 mL of acidified Fluka water (pH = 2) to the column. The HLB column was dried, and then the species adsorbed on the column were eluted with 6 mL MeOH. The organics in this effluent are referred to as humic-like

substances with an acidic nature in WSOM (HULIS-a), because the pH dependence of the absorption can be explained by different degrees of dissociation of carboxylic groups therein. In the case of organic acids, their acid ionization constants pK_a may range from 2 to 7. The effluent in this step was collected in 15-mL pre-cleaned sample bottles. According to the adsorption mechanism of HLB, this fraction should contain highly polar species. We refer to organics in this fraction as high polarity (HP-) WSOM.

To evaluate the recovery of organics in SPE, the concentrations of WSOM directly determined using HR-AMS and the concentrations of the sum of HULIS-n, HULIS-a and HP-WSOM were compared. The result shows that the recoveries of the SPE procedure were 106 ± 8% (r^2 = 0.94; n = 12) for WSOM and 105 ± 19% (r^2 = 0.96; n = 12) for WSOC, indicating that most of the WSOM were recovered. Although different organics may have different RIE in the AMS analysis (1.4 for atmospheric particulate organics and 1.2 for hydrocarbons)[9], WSOM and the sum of three components in WSOM probably contain nearly the same type of organics, and thus the uncertainty of the above values of recovery may not be greatly influenced by the uncertainty of RIE.

S5. FT-IR data analysis

For the quantitative analysis of the chemical functional groups using diffuse reflectance FTIR spectroscopy, DRIFTS data were represented by Kubelka-Munk (K-M) units:[10]

$$f(R_\infty) = \frac{k}{s} = \frac{(1-R_\infty)^2}{2R_\infty} \propto \frac{\varepsilon c}{s} \tag{3}$$

where R_∞ is the intensity of scattered IR divided by that of the incident radiation, k is the sample absorption, s is the scattering coefficient, ε is the absorptivity, and c is the concentration of the material that absorbs IR. The Kubelka-Munk conversion was performed using matched software (JASCO).

For the quantification of organic functional groups, the FTIR spectra were integrated in a manner analogous to that described in previous reports.[11-14] A linear combination of a series of Gaussian distribution functions was used to represent the absorption of multiple functional groups (alcohol CO-H, aromatic C-H, alkene C-H, alkane C-H, carbonyl C=O, amines C-NH$_2$, organonitrate C-ONO$_2$ and unidentified groups in Table S2), and peak patterns of carboxylic COH (from Takahama et al., 2013) and ammonium (from NH$_4$NO$_3$) were used to represent their absorption at the 1500−4000 cm^{-1} region. A least squares optimization method for the determination of peak parameters was performed to minimize the error:

$$Error = (Abs(\lambda) - F(\lambda))^2$$
$$F(\lambda) = \sum_i \alpha_i \cdot C_i(\lambda) + \sum_j \beta_j \cdot \exp[-\frac{(\lambda - \mu_j)^2}{2 \cdot \sigma_j^2}] \tag{4}$$

where $Abs(\lambda)$ is the observed absorption in the KM unit; $F(\lambda)$ is the fitted curve; $C_i(\lambda)$ is the line shapes for carboxylic COH and ammonium N-H; α_i is the scaling factor; β, μ and σ are parameters of the Gaussian function; and j denotes different chemical functional groups.

The areas of fitted peaks were used to quantify different functional groups. The peak area of non-carboxylic C=O was calculated as the total peak area of carbonyl C=O minus the peak areas of carboxylic COOH at the 1710−1740 cm^{-1} region.[14] Similarly, the peak area of amine C-NH$_2$ at the 1630−1640 cm^{-1} region was calculated as the total peak area minus the peak area of

organonitrate $C-ONO_2$.[13] Organonitrate $C-ONO_2$ was quantified directly from the peak area at the 1265−1300 cm^{-1} region.[11] The relative contents of different chemical groups in organics were also used to determine the elemental ratios and OM/OC in accordance with Takahama et al.[14] The absolute mass concentrations of the fractionated organics were not quantified from the FT-IR data. Instead, relative contents of different chemical groups in fractionated organics were calculated based on previously reported absorptivity in Table S2.

The uncertainty of quantification of transmittance FT-IR spectroscopy were reported to be 21% and 33% for carboxylic COOH and ketonic C=O, respectively, and 5%−21% for other functional groups.[14-17] The reproducibility of the functional group analysis based on the FT-IR analysis in this study was examined by the extraction and the FT-IR analysis of an identical aerosol sample (an extra filter sample) three times; the RSD of the mass percentage of the C-OH, COOH, C=O, $C-NH_2$, $C-ONO_2$, and C-H groups of WISOM, HULIS-n and HULIS-a were, respectively, 7−32%, 5−13%, 2−32%, 51−76%, 11−19%, and 1−11%. The RSD of O/C, H/C, and OM/OC from the FT-IR analysis were in the ranges of 6.3−12.2%, 0.5−0.9%, and 0.7−5.4%, respectively (n = 3 for WISOM, HULIS-n and HULIS-a, respectively). The RSD of the FT-IR-derived mass of organics (in ∑(KM-area/absorptivity)) for WISOM, HULIS-n and HULIS-a were 13.0%, 14.1% and 5.0%, respectively (n = 3).

S6. Assessment of the possible influence of ammonia to the analysis of HULIS

A possible change in the composition of the organic compounds by the elution using

methanol containing 2 wt% ammonia was assessed. For the assessment, we used 4 ml MeOH instead of 2 mL of MeOH containing 2 wt% ammonia to elute HULIS from Oasis HLB cartridges in the first step (Figure S1). This MeOH extractable HULIS is hereafter referred to as HULIS-M. The HULIS-M eluent was equally divided into two 15 ml vial bottles, and 2 ml of MeOH containing 4 wt% ammonia was mixed to one of the splits, fully dried under a nitrogen flow and redissolved with 2 ml of MeOH (referred to as HULIS-M-A). The same analysis method described in the experimental section was followed to obtain the HR-AMS and FT-IR spectra of HULIS-M and HULIS-M-A, and the results were compared to those based on the original method.

Figure S7 presents the results of the chemical structures for HULIS-M and HULIS-M-A from HR-AMS and FT-IR spectra. First, no substantial differences in the relative intensity of $C_xH_yN_z^+$ ions and other ion groups in the HR-AMS spectra were observed for HULIS-M and HULIS-M-A (difference: <2% of total organic signals) or in the element ratios (difference: <8%). Furthermore, no substantial difference in the relative intensity of absorption peaks at approximately 1720, 1630 and 1589 cm^{-1} in the FT-IR spectra were observed for HULIS-M or HULIS-M-A (<10%). The compounds that contributed to the peaks at 1630 and 1589 cm^{-1} should have originally been present in aerosol organic matter because these peaks in the FT-IR spectra of HULIS-M, which is not mixed with ammonia, were intense. These results suggest that the composition of HULIS did not change significantly with the use of methanol containing 2 wt% ammonia for elution. This result is in agreement with that suggested by Lin et al.: They confirmed that the aqueous ammonia in MeOH did not lead to significant artifacts in the molecular-level determination of

HULIS by HR-ESI-MS.[8] Note that we observed a peak increase in the absorption at 3130 cm^{-1} in the FT-IR spectra of HULIS-M-A. This absorption was caused by the associated ammonia that remained in the samples. The absorption did not affect the quantification of chemical functional groups because this peak could be clearly distinguished from nearby peaks of the C-H and C-OH groups with the use of the peak patterns of ammonium from NH_4NO_3 for fitting.

References:

(1) Psichoudaki, M. and Pandis, S. N. Atmospheric Aerosol Water-Soluble Organic Carbon Measurement: A Theoretical Analysis. *Environ. Sci. Technol.* **2013**, *47* (17), 9791−9798.

(2) Kim, K.H.; Sekiguchi, K.; Kudo, S.; Kinoshita, M.; Sakamoto, K. Carbonaceous and ionic components in ultrafine and fine particles at four sampling sites in the vicinity of roadway intersection. *Atmos. Environ.* **2013,** *74*, 83–92.

(3) Fana, X.; Brookb, J.R.; Mabury, S.A. Measurement of organic and elemental carbon associated with PM2.5 during Pacific 2001 study using an integrated organic gas and particle sampler. *Atmos. Environ.* **2004**, *38*, 5801–5810.

(4) Cheng, Y.; He, K.B.; Duan, F.K.; Zheng, M.; Ma, Y. L.; Tan, J.H. Positive sampling artifact of carbonaceous aerosols and its influence on the thermal-optical split of OC/EC. *Atmos. Chem. Phys.,* **2009**, *9*, 7243–7256.

(5) Dabek-Zlotorzynska, E.; Dann, T.F.; Martinelango, P.K.; Celo, V.; Brook, J.R.; Mathieu, D.; Ding, L.; Austin, C.C. Canadian National Air Pollution Surveillance (NAPS) PM2.5 speciation program: Methodology and PM2.5 chemical composition for the years 2003–2008. *Atmos. Environ.* **2011**, *45*, 673−686.

(6) Kim, B.M.; Cassmassi, J.; Hogo,H.; Zeldin, M.D. Positive Organic Carbon Artifacts on Filter Medium During PM2.5 Sampling in the South Coast Air Basin. *Aerosol Science and Technology* **2001**, *34*, 35–41.

(7) Varga, B.; Kiss, G.; Ganszky, I.; Gelencsér, A.; Krivácsy, Z. Isolation of water-soluble organic matter from atmospheric aerosol. *Talanta* **2001**, *55* (3), 561–572.

(8)   Lin, P.; Rincon, A. G.; Kalberer, M.; Yu, J. Elemental Composition of HULIS in the Pearl River Delta Region, China: Results Inferred from Positive and Negative Electrospray High Resolution Mass Spectrometric Data. *Environ. Sci. Technol.* **2012**, *46* (14), 7454−7462.

(9)   Jimenez, J. L.; Jayne, J. T.; Shi, Q.; Kolb, C. E.; Worsnop, D. R.; Yourshaw, I.; Seinfeld, J. H.; Flagan, R. C.; Zhang, X.; Smith, K. A.; Morris, J. W.; Davidovits, P. Ambient aerosol sampling using the Aerodyne Aerosol Mass Spectrometer. *J. Geophys. Res.* **2003**, *108* (D7), 1–13.

(10) Sirita, J.; Phanichphant, S.; Meunier, F. C. Quantitative Analysis of Adsorbate Concentrations by Diffuse Reflectance FT-IR. *Anal. Chem.* **2007**, *79* (10), 3912–3918.

(11) Sax, M.; Zenobi, R.; Baltensperger, U.; Kalberer, M. Time Resolved Infrared Spectroscopic Analysis of Aerosol Formed by Photo-Oxidation of 1,3,5-Trimethylbenzene and α-Pinene. *Aerosol Science and Technology* **2005**, *39* (9), 822–830.

(12) Russell, L. M.; Takahama, S.; Liu, S.; Hawkins, L. N.; Covert, D. S.; Quinn, P. K.; Bates, T. S. Oxygenated Fraction and Mass of Organic Aerosol from Direct Emission and Atmospheric Processing Measured on the R/V Ronald Brown During TEXAQS/GoMACCS 2006. *J. Geophys. Res.* **2009**, *114* (D7), 1–15.

(13) Day, D. A.; Liu, S.; Russell, L. M.; Ziemann, P. J. Organonitrate group concentrations in submicron particles with high nitrate and organic fractions in coastal southern California. *Atmos. Environ.* **2010**, *44* (16), 1970−1979.

(14) Takahama, S.; Johnson, A.; Russell, L. M. Quantification of Carboxylic and Carbonyl Functional Groups in Organic Aerosol Infrared Absorbance Spectra. *Aerosol Science and Technology* **2013**, *47* (3), 310–325.

(15) Russell, L. M. Aerosol Organic-Mass-to-Organic-Carbon Ratio Measurements. *Environ. Sci. Technol.* **2003**, *37* (13), 2982–2987.

(16) Maria, S. F.; Russell, L. M.; Turpin, B. J.; Porcja, R. J.; Campos, T. L.; Weber, R. J.; Huebert, B. J. Source signatures of carbon monoxide and organic functional groups in Asian Pacific Regional Aerosol Characterization Experiment (ACE-Asia) submicron aerosol types. *J. Geophys. Res.* **2003**, *108* (D23), 1–5.

(17) Gilardoni, S.; Russell, L. M.; Sorooshian, A.; Flagan, R. C.; Seinfeld, J. H.; Bates, T. S.; Quinn, P. K.; Allan, J.

D.; Williams, B.; Goldstein, A. H.; Onasch, T. B.; Worsnop, D. R. Regional variation of organic functional groups in aerosol particles on four U.S. east coast platforms during the International Consortium for Atmospheric Research on Transport and Transformation 2004 campaign. *J. Geophys. Res.* **2007**, *112* (D10), 1–11.

(18) Chirico, R.; Prevot, A. S. H.; DeCarlo, P. F.; Heringa, M. F.; Richter, R.; Weingartner, E.; Baltensperger, U. Aerosol and trace gas vehicle emission factors measured in a tunnel using an Aerosol Mass Spectrometer and other on-line instrumentation. *Atmos. Environ.* **2011**, *45* (13), 2182–2192.

(19) Mohr, C.; Decarlo, P. F.; Heringa, M. F.; Chirico, R.; Slowik, J. G.; Richter, R.; Reche, C.; Alastuey, A.; Querol, X.; Seco, R.; Peñuelas, J.; Jiménez, J. L.; Crippa, M.; Zimmermann, R.; Baltensperger, U.; Prévôt, A. S. H. Identification and quantification of organic aerosol from cooking and other sources in Barcelona using aerosol mass spectrometer data. *Atmos. Chem. Phys.* **2012**, *12*, 1649–1665.

(20) Lechner, M.; Ulbrich, I.M.; Jimenez, J.L. High-Resolution AMS Spectral Database. URL: http://cires.colorado.edu/jimenez-group/HRAMSsd/.

(21) Gilardoni, S.; Liu, S.; Takahama, S.; Russell, L. M.; Allan, J. D.; Steinbrecher, R.; Jimenez, J. L.; Carlo, P. F. D.; Dunlea, E. J.; Baumgardner, D. Characterization of organic ambient aerosol during MIRAGE 2006 on three platforms. *Atmos. Chem. Phys.* **2009**, *9*, 5417–5432.

(22) Maria, S. F.; Russell, L. M.; Turpin, B. J.; Porcja, R. J. FTIR measurements of functional groups and organic mass in aerosol samples over the Caribbean. *Atmos. Environ.* **2002**, *36* (33), 5185–5196.

(23) Allen, D. T.; Palen, E. J.; Haimov, M. I.; Hering, S. V.; Young, J. R. Fourier-Transform Infrared-Spectroscopy of Aerosol Collected In A Low-pressure Impactor (lpi/ftir)—Method Development and Field Calibration. *Aerosol Sci. Technol.* **1994**, *21* (4), 325–342.

(24) Colthup, N.B.; Daly, L.H.; Wiberley, S.E. Introduction to infrared and Raman spectroscopy, Academic press: New York and London, 1964.
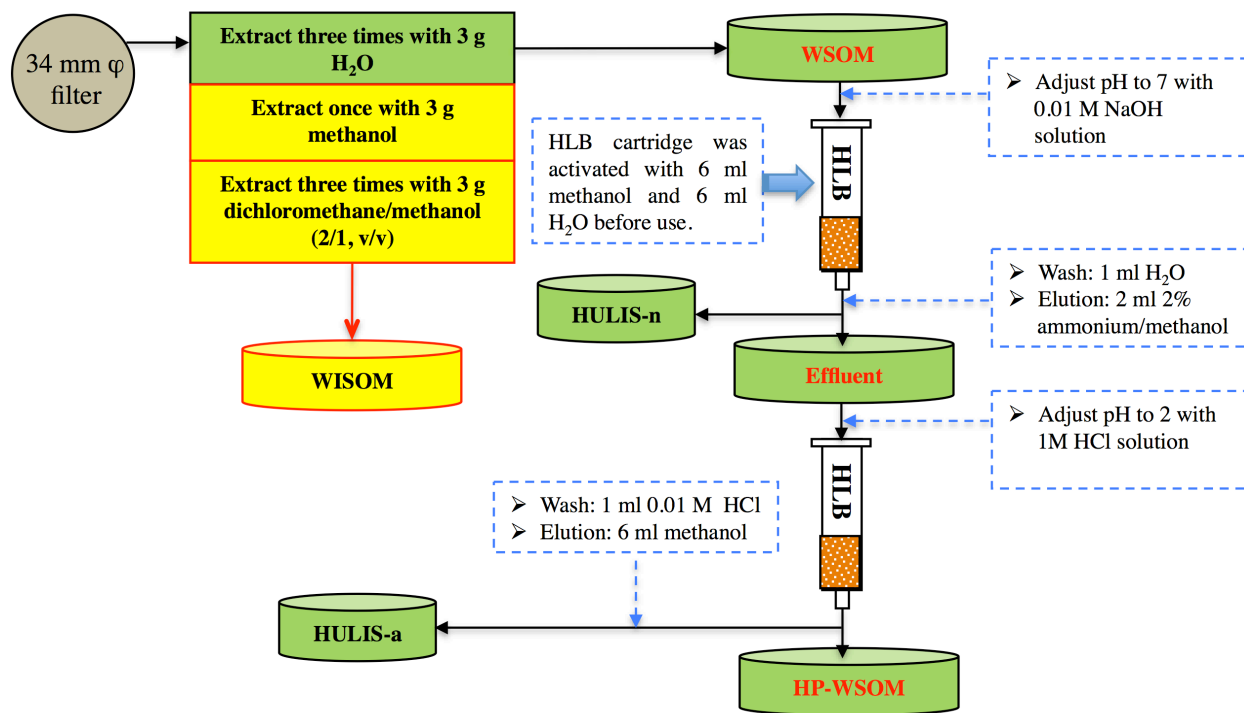
Figure S1. The procedure of solvent extraction and SPE for fractionation of organics in TSP samples.
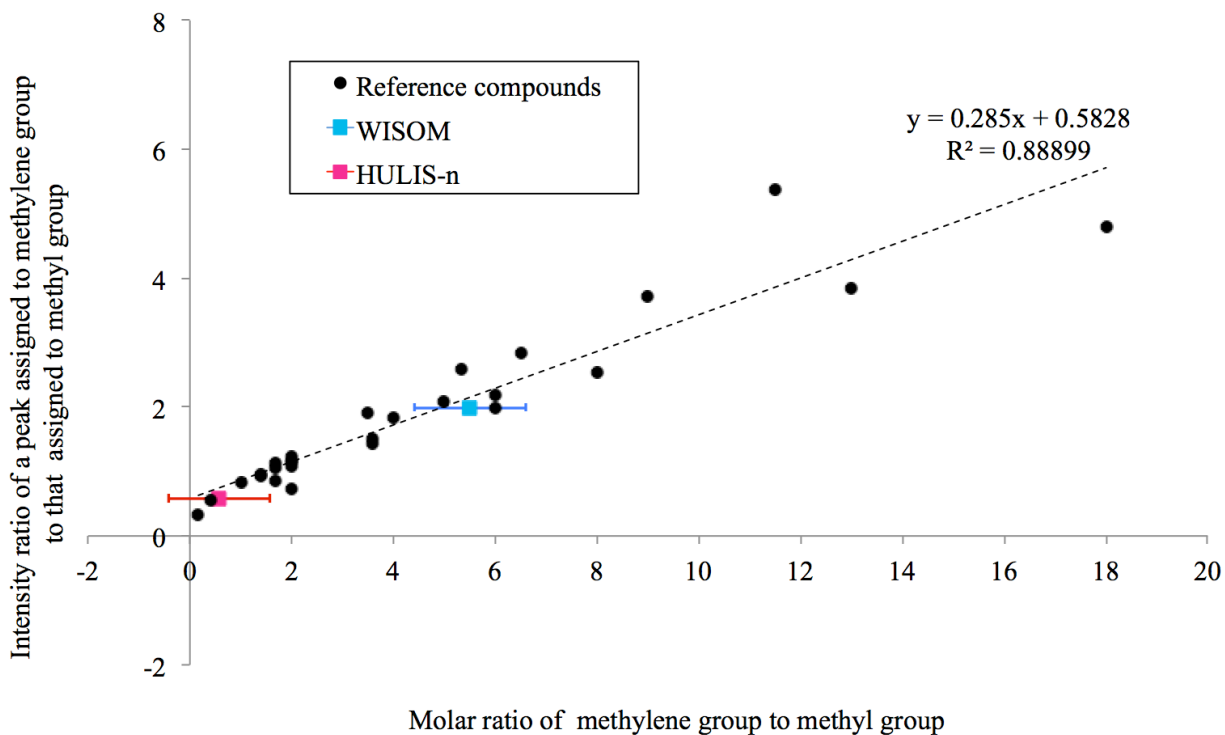
Figure S2. The relationship between the molar ratio of -CH$_2$- group to -CH$_3$ group and the intensity ratio of their corresponding infrared peaks at ~2960 and ~2930 cm^{-1}, respectively.[24]
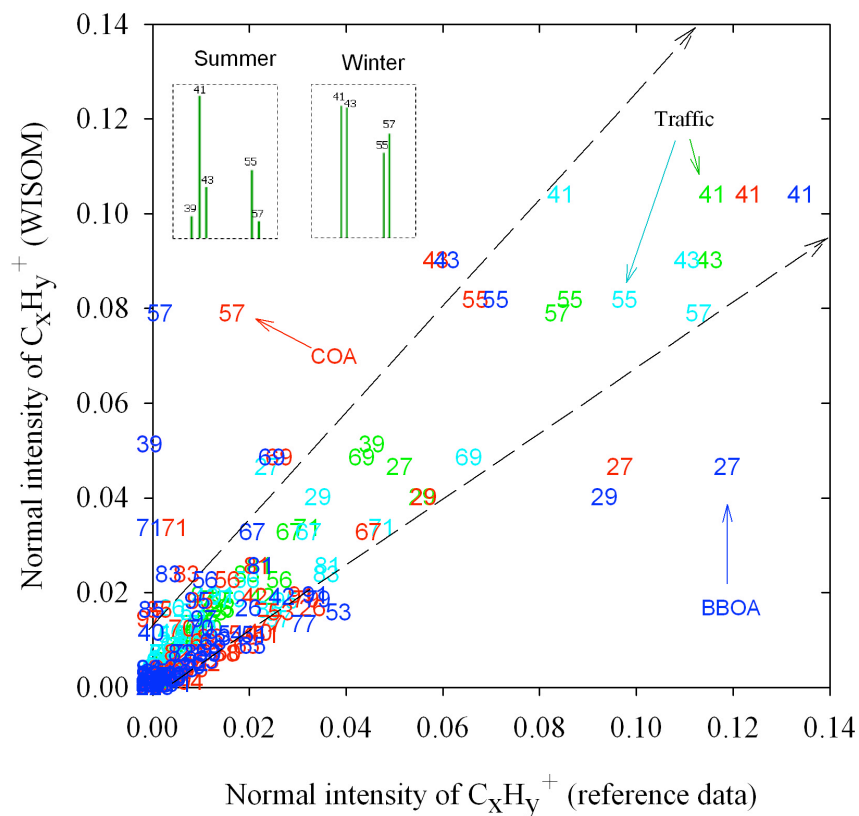
Figure S3. Plots of $C_xH_y^+$ ions from HR-ToF-AMS spectra of different POA versus those of WISOM in this study, in the range of m/z upto 100. Green: traffic emissions OA in a tunnel;[18] cyan: HOA identified as traffic emissions from PMF; red: COA from PMF; blue: BBOA from PMF.[19] The spectra are from URL: http://cires.colorado.edu/jimenez-group/HRAMSsd/.[20]
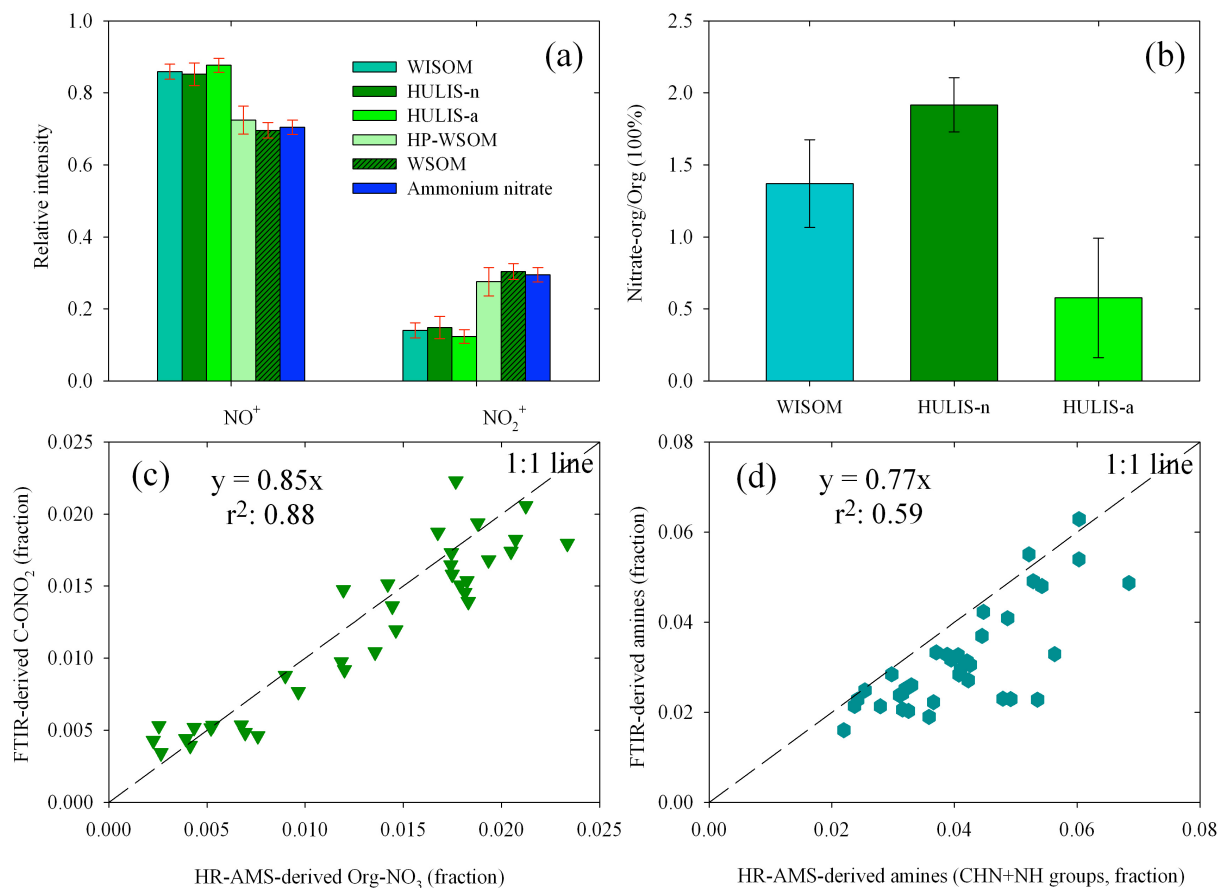
Figure S4. (a) The ratio of NO^+ (m/z 30) to NO_2^+ (m/z 46) in the HR-AMS spectra of the extracts (n = 12) and ammonium nitrate standard (n = 5). (b) Estimated mass percentages of organic nitrates (NO_3) in WISOM, HULIS-n, and HULIS-a (from HR-AMS). (c and d) Estimated mass percentages of organic nitrates and amines from FT-IR spectra versus HR-AMS-derived mass percentages of (c) NO_3 and (d) CHN + NH groups of organics.
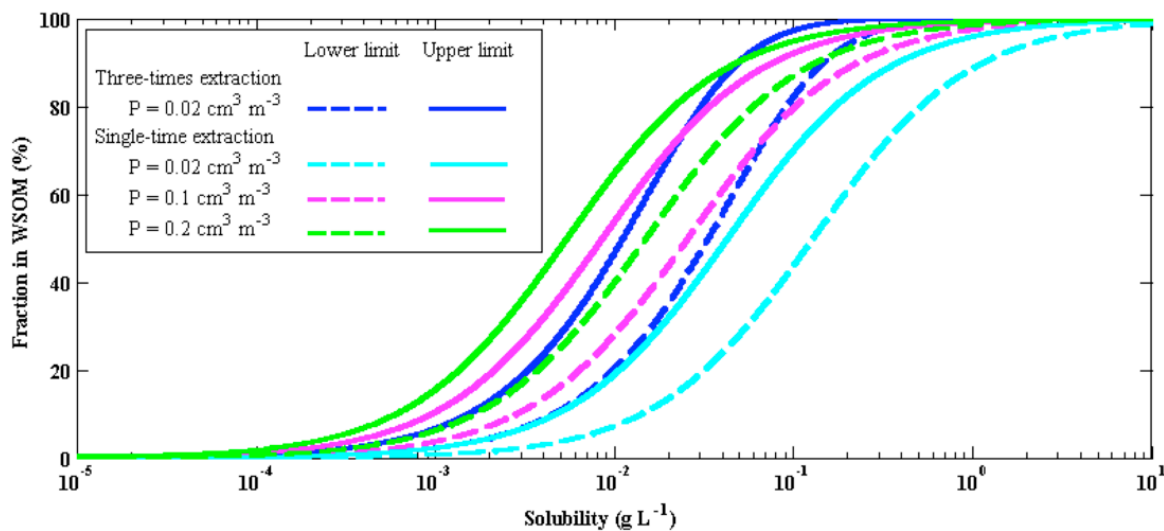
Figure S5. Efficiency of water extraction of organics as a function of their solubility in water under various extraction conditions. The lower and upper limits were calculated with the assumptions of maximum (3 μg m^{-3}) and minimum (1.5 μg m^{-3}) concentrations of WISOM, respectively.
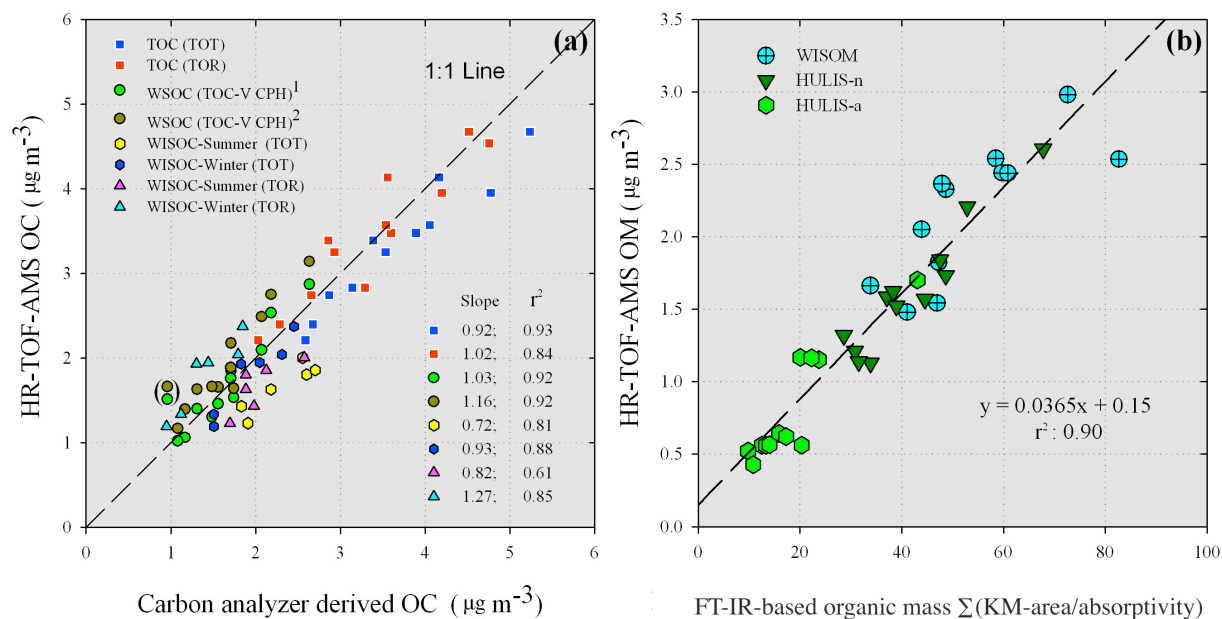
Figure S6. (a) OC concentrations from the HR-AMS plotted against those from the TOC analyzer. WSOC[1] and WSOC[2] in the vertical axis are from HR-AMS-derived WSOM and from HULIS-n, HULIS-a, and HP-WSOM derived from HR-AMS, respectively. The plot for the sample influenced by marine aerosol (8/30-9/3) largely deviated from the 1:1 line and is shown in parenthesis. (b) The organic mass concentrations from HR-AMS plotted against the mass of organics (in $\sum$(KM-area/absorptivity)) quantified from identified peaks in the FT-IR spectra.
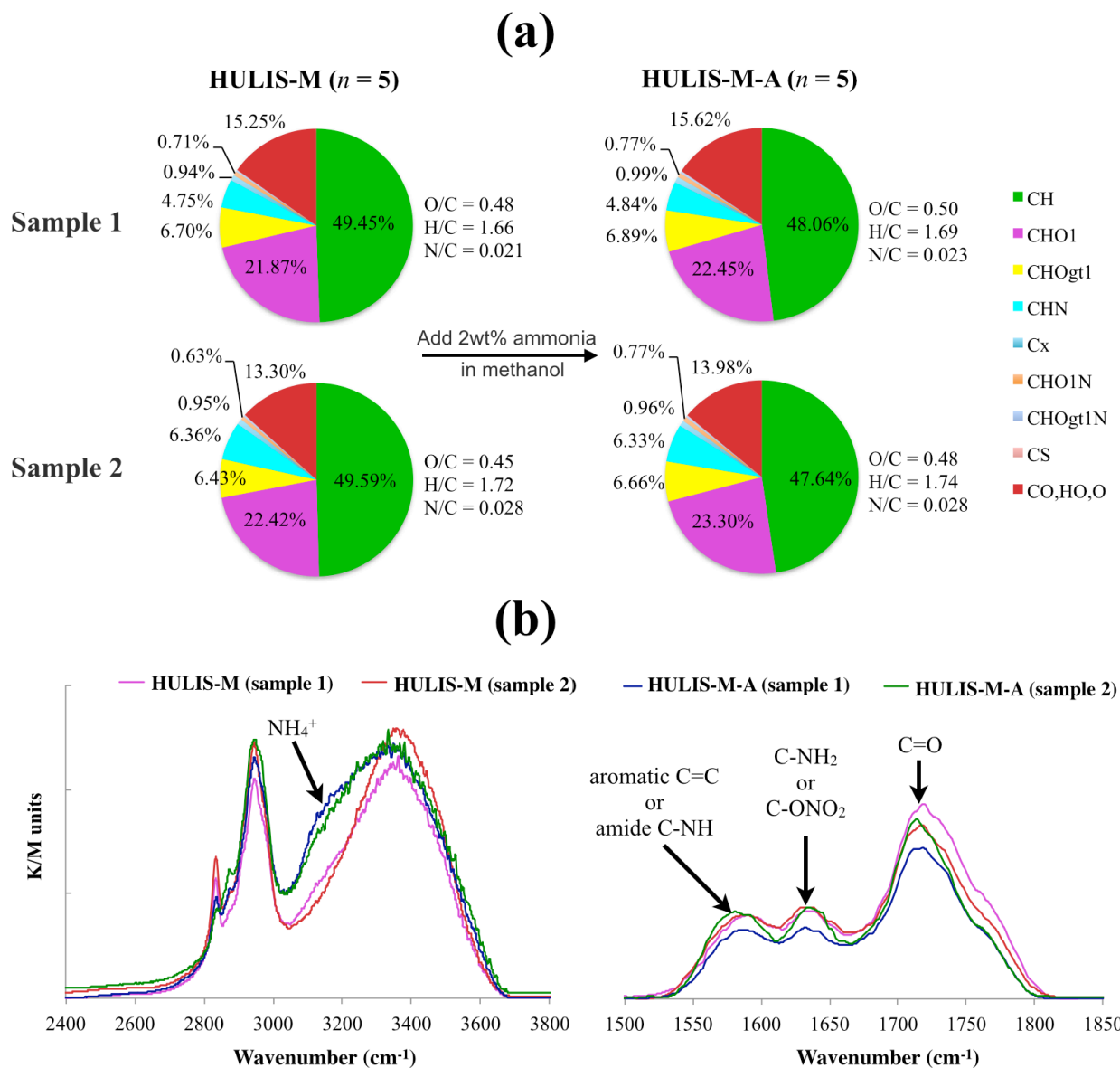
Figure S7. (a) Element ratios and relative intensity of ion groups in the HR-AMS spectra of MeOH-elutable HULIS (HULIS-M) and HULIS-M after the treatment by the addition of methanol containing 2 wt% ammonia (HULIS-M-A). (b) The absorption peaks of the FT-IR spectra of HULIS-M and HULIS-M-A.

Table S1. Summary of the abundance s of methyl and methylene groups in reference compounds and extracted fractions, and the corresponding infrared peak ratios

Reference compounds and extracted fractions	Number of -CH_3	Number of -CH_2-	Molar ratio of -CH_2- to -CH_3	Intensity ratio of a peak assigned to –CH_3 (~2930 cm^{-1})[24] to that assigned to -CH_2- (~2960 cm^{-1})[24]
3-Hexanol, 2,2,5,5-tetramethyl- ($C_{10}H_{22}O$)	6	1	0.2	0.34 [a]
Heptane, 2,4,6-trimethyl- ($C_{10}H_{22}$)	5	2	0.4	0.54 [a]
Octane, 2,3-dimethyl- ($C_{10}H_{22}$)	4	4	1.0	0.84 [a]
Dodecane, 2,6,10-trimethyl- ($C_{15}H_{32}$)	5	7	1.4	0.93 [a]
Dodecane, 2,6,11-trimethyl- (C15H32)	5	7	1.4	0.96 [a]
Hexadecane, 2,6,11,15-tetramethyl- ($C_{20}H_{42}$)	6	10	1.7	1.05 [a]
3-Nonanol, 2-methyl- ($C_{10}H_{22}O$)	3	5	1.7	1.13 [a]
3-Octanol, 6-ethyl- ($C_{10}H_{22}O$)	3	5	1.7	0.85 [a]
Nonane, 3-methyl- ($C_{10}H_{22}$)	3	6	2.0	1.23 [a]
Octane, 3-ethyl- ($C_{10}H_{22}$)	3	6	2.0	1.15 [a]
Squalane ($C_{30}H_{62}$)	8	16	2.0	1.15 [a]
1-Dodecanol, 3,7,11-trimethyl- ($C_{15}H_{32}O$)	4	8	2.0	1.08 [a]
4-Heptanol, 4-propyl- ($C_{10}H_{22}O$)	3	6	2.0	0.74 [a]
2-Decanone ($C_{10}H_{20}O$)	2	7	3.5	1.92 [a]
heptadecane, 6,12-diethyl-9-pentyl- ($C_{26}H_{54}$)	5	18	3.6	1.50 [a]
heptadecane, 6,9,12-tripropyl- ($C_{26}H_{54}$)	5	18	3.6	1.43 [a]
Decane ($C_{10}H_{22}$)	2	8	4.0	1.85 [a]
Hexadecane, 6,11-dipentyl- ($C_{26}H_{54}$)	4	20	5.0	2.08 [a]
Nonadecane, 2-methyl- ($C_{20}H_{42}$)	3	16	5.3	2.59 [a]
2-Pentadecanol ($C_{15}H_{32}O$)	2	12	6.0	1.99 [a]
8-Pentadecanone ($C_{15}H_{30}O$)	2	12	6.0	2.18 [a]
Pentadecane ($C_{15}H_{32}$)	2	13	6.5	2.83 [a]
Decanal ($C_{10}H_{20}O$)	1	8	8.0	2.55 [a]
Eicosane ($C_{20}H_{42}$)	2	18	9.0	3.71 [a]
Pentacosane $C_{25}H_{52}$	2	23	11.5	5.37 [a]
n-Pentadecanol ($C_{15}H_{32}O$)	1	13	13.0	3.85 [a]
1-Eicosanol ($C_{20}H_{42}O$)	1	18	18.0	4.79 [a]
WISOM in this study	n/a	n/a	5.5±1.1 [b]	1.89±0.07 [b]
HULIS-n in this study	n/a	n/a	0.57±1.0 [b]	0.48±0.01 [b]

[a] From the infrared spectra in http://webbook.nist.gov/chemistry/

[b] Mean ± SD, n = 12.

Table S2. Fitting parameters and absorptivity of chemical groups.

Peak no.	Functional group	Constraints		1/Absorptivity [a]
		μ (cm^{-1})	σ (cm^{-1})	
1	Carboxylic COH	Lineshape; 2400−3400 [d]		0.015 [d, e]
2	Ammonium NH$_4$ [b]	Lineshape; 2500−3500 [c]		-
3	Alcohol COH—1	3400−3600	30−100	0.057 [d, e, f]
4	Alcohol COH—2	3200−3350	30−75	0.057 [d, e, f]
5	Unidentified—1[2]	3136−3142	10−20	-
6	Unidentified—2	3070−3076	10−20	-
7	Aromatic CH	3030−3070	3.5	8.7 [d, e]
8	Unidentified—3	3014−3008	10−25	-
9	Alkene CH	2980−3010	3.5	3.8 [d, e]
10	Alkane (CH$_3$) CH—1	2940−2960	5−15	0.6 [e, f]
11	Alkane (CH$_2$) CH—2	2920−2930	10−40	0.6 [e, f]
12	Alkane (CH$_3$) CH—3	2873−2886	10−40	0.6 [e, f]
13	Alkane (CH$_2$) CH—4	2830−2858	5−25	0.6 [e, f]
14	Alkane CH—5	2805−2811	10−20	0.6 [e, f]
15	Carbonyl CO	1710−1740	10−40	0.067 [e, f, j]
	Carboxylic CO			0.034 [l]
16	Amine CNH$_2$—1	1627−1640	5−30	0.112 [d, e, g, h]
	Organonitrate CONO$_2$—1			0.037 [j, k]
17	Amine CNH$_2$—2	1587−1610	3−30	-
18	Organonitrate CONO$_2$—2	1265−1300	-	0.075 [k]
19	Organonitrate CONO$_2$—3	850−870	3−30	-

[a] Absorptivity is the unit of peak area (in absorbance) per micromole of functional group.

[b] This peak may be contributed by amines.

[c] An absorption profile of ammonium from NH$_4$NO$_3$.

[d] Takahama et al., 2013;[14] [e] Russell et al., 2009;[12] [f] Gilardoni et al., 2009;[21] [g] Gilardoni et al., 2007;[17] [h] Maria et al., 2002;[22] [l] Allen et al., 1994;[23] [j] Day et al., 2010;[13] [k] Sax et al., 2005.[11]

Table S3. The raw data and statistics of concentrations of inorganic and organic species in total suspended particulates over Nagoya, Japan.

(μg m^{-3})	WISOM	WSOM	HULIS-n	HULIS-a	HP-WSOM	EOM	EOC	Oxalic	EC	nss-SO$_4^{2-}$	NO$_3^-$	NH$_4^+$	Cl$^-$	Na$^+$	K$^+$	nss-Ca^{2+}	Mg^{2+}
7/26-8/2, 2011	2.05	3.67	1.58	1.15	1.26	5.72	3.23	0.40	1.40	4.80	0.60	0.74	0.10	0.96	0.18	0.34	0.14
8/2-8/9, 2011	2.54	5.17	2.20	1.16	1.61	7.71	4.21	0.49	2.11	4.40	1.64	0.40	0.08	1.27	0.20	0.69	0.19
8/9-8/16, 2011	2.32	5.46	2.60	1.70	1.21	7.79	4.33	0.50	2.10	8.12	0.37	1.51	0.02	0.77	0.23	0.62	0.14
8/16-8/23, 2011	2.36	4.09	1.73	1.16	1.76	6.46	3.67	0.52	1.88	6.18	1.00	1.33	0.11	0.63	0.17	0.53	0.11
8/23-8/30, 2011	1.82	2.96	1.21	0.64	1.24	4.78	2.63	0.50	1.57	5.10	1.96	0.70	0.06	1.40	0.16	0.46	0.20
8/30-9/6, 2011	1.54	3.28	1.12	0.56	1.44	4.82	2.52	0.27	1.17	3.01	0.69	0.01	2.56	2.44	0.14	0.42	0.30
12/27, 2011-1/4, 2012	2.44	2.68	1.57	0.62	0.69	5.12	3.15	0.09	1.91	2.73	2.40	1.24	0.73	0.58	0.14	0.31	0.06
1/4-1/10, 2012	1.66	1.99	1.31	0.52	0.58	3.66	2.23	0.07	1.34	2.31	1.79	1.16	0.99	0.57	0.10	0.25	0.05
1/10-1/17, 2012	2.43	2.43	1.62	0.56	0.70	4.86	3.04	0.11	1.76	3.55	2.61	1.59	0.88	0.50	0.15	0.44	0.06
1/17-1/24, 2012	2.98	3.18	1.84	0.56	0.85	6.16	3.86	0.15	2.13	2.33	3.88	1.57	0.71	0.32	0.14	0.46	0.03
1/24-1/31, 2012	1.47	1.89	1.13	0.42	0.43	3.37	2.05	0.08	1.42	2.88	2.14	1.24	0.25	0.26	0.16	0.29	0.04
1/31-2/7, 2012	2.53	2.88	1.52	0.56	0.81	5.42	3.34	0.14	1.89	3.89	3.62	2.03	1.21	0.67	0.16	0.40	0.07
Minimum for all	1.47	1.89	1.12	0.42	0.43	3.37	2.05	0.07	1.17	2.31	0.37	0.01	0.02	0.26	0.10	0.25	0.03
Maximum for all	2.98	5.46	2.60	1.70	1.76	7.79	4.33	0.52	2.13	8.12	3.88	2.03	2.56	2.44	0.23	0.69	0.30
Average (SD) for summer/early-autumn	2.10 (0.34)	4.10 (0.92)	1.74 (0.52)	1.06 (0.37)	1.42 (0.20)	6.21 (1.22)	3.43 (0.70)	0.45 (0.08)	1.71 (0.35)	5.27 (1.58)	1.04 (0.57)	0.78 (0.51)	0.49 (0.92)	1.25 (0.59)	0.18 (0.02)	0.51 (0.12)	0.18 (0.06)
Average (SD) for winter	2.25 (0.52)	2.51 (0.46)	1.50 (0.22)	0.54 (0.05)	0.68 (0.13)	4.77 (0.97)	2.95 (0.62)	0.11 (0.02)	1.74 (0.27)	2.95 (0.59)	2.74 (0.76)	1.47 (0.29)	0.80 (0.29)	0.48 (0.14)	0.14 (0.02)	0.36 (0.07)	0.05 (0.01)
Average (SD) for all	2.18 (0.44)	3.31 (1.08)	1.62 (0.42)	0.80 (0.37)	1.05 (0.41)	5.49 (1.32)	3.19 (0.71)	0.28 (0.18)	1.72 (0.31)	4.11 (1.66)	1.89 (1.08)	1.13 (0.54)	0.64 (0.70)	0.87 (0.57)	0.16 (0.03)	0.44 (0.12)	0.12 (0.07)

Table S4. The ranges of the total extracted masses and the mass concentrations of organics from HR-AMS and FT-IR, and the corresponding uncertainty of the quantification of organic masses.

	Organics mass in respective extracts (μg)	Mass concentration of organics in respective extracts (%)	Uncertainty [b]
HR-AMS	80−930	0.0008−0.0110 (in solution)	0.5%−10.8%
FT-IR	159−970	0.08−0.49 (with KBr)	5.0%−14.1%

[a] From repeated quantification of organics masses for WISOM, WSOM, HULIS-n, HULIS-a, and HP-WSOM.

Table S5. The operational definitions of WSOM, WISOM, HULIS-n, HULIS-a and HP-WSOM components.

	Operational definitions
WSOM	Organic matter extracted from filter samples with water for three times
WISOM	Organic matter extracted with methanol for once and subsequently with dichloromethane/methanol (2/1, v/v) for three times after the extraction of WSOM with water
HULIS-n	Organic matter that adsorbed on an Oasis HLB cartridge from WSOM with the condition of pH = 7 and was eluted with the solvent of methanol containing 2 wt% of ammonia
HULIS-a	Organic matter that adsorbed on an Oasis HLB cartridge under the condition of pH = 2 and was eluted with methanol, among organic matter in the effluent of the first step of the HLB extraction
HP-WSOM	Organic matter in the effluent of the second step of the HLB extraction

Table S6. Mass fractions of functional groups in WISOM, HULIS-n and HULIS-a (from FT-IR spectra, $n = 12$).

Fraction	Functional group (%, mean ± SD)					
	C–H	C–OH	COOH	C=O	C–NH$_2$	C–ONO$_2$
WISOM	76.9 ± 4.4	10.2 ± 2.2	1.9 ± 0.4	7.0 ± 1.8	2.4 ± 0.4	1.3 ± 0.4
HULIS-n	46.6 ± 4.4	35.1 ± 3.9	3.6 ± 17.5	8.7 ± 16.1	4.0 ± 34.8	1.6 ± 11.1
HULIS-a	32.4 ± 5.6	35.8 ± 11.3	9.8 ± 17.3	18.4 ± 14.5	2.8 ± 24.4	0.4 ± 13.1

Table S7. Mass fractions of ion groups in the HR-AMS spectra of different organic fractions ($n = 12$).

Fraction	Ion group (%, mean ± SD)							
	CH	CO, O, OH	CHO_1	$CHO_{>1}$	CHN	CHO_1N	$CHO_{>1}N$	CS
WISOM	79.1 ± 2.0	3.9 ± 0.8	10.3 ± 1.0	3.0 ± 0.1	1.6 ± 0.1	0.7 ± 0.0	0.6 ± 0.0	0.1 ± 0.0
WSOM	32.5 ± 4.0	32.5 ± 6.9	18.6 ± 2.2	6.9 ± 1.2	5.4 ± 1.0	1.8 ± 0.2	0.9 ± 0.1	0.5 ± 0.2
HULIS-n	47.9 ± 0.9	13.0 ± 1.4	25.0 ± 0.5	6.6 ± 0.8	5.2 ± 0.7	1.0 ± 0.1	0.8 ± 0.1	0.1 ± 0.0
HULIS-a	35.2 ± 1.4	26.5 ± 3.0	24.2 ± 0.8	8.6 ± 0.4	3.6 ± 0.8	0.8 ± 0.1	0.8 ± 0.1	0.1 ± 0.0
HP-WSOM	23.9 ± 2.1	36.5 ± 3.2	22.5 ± 3.3	5.4 ± 0.6	9.1 ± 2.6	0.8 ± 0.1	0.7 ± 0.3	0.5 ± 0.5

Table S8. The O/C, H/C, and OM/OC of organics in different fractions (mean ± SD, $n = 12$).

Fraction	FT-IR			HR-AMS		
	O/C[a]	H/C[a]	OM/OC[b]	O/C[a]	H/C[a]	OM/OC[b]
WISOM	0.12 ± 0.02	1.83 ± 0.04	1.31 ± 0.02	0.14 ± 0.03	1.8 ± 0.02	1.36 ± 0.05
WSOM	0.76 ± 0.10	1.39 ± 0.06	2.17 ± 0.13			
HULIS-n	0.41 ± 0.02	1.66 ± 0.02	1.71 ± 0.03	0.45 ± 0.02	1.76 ± 0.03	1.80 ± 0.12
HULIS-a	0.67 ± 0.03	1.52 ± 0.05	2.04 ± 0.03	0.66 ± 0.03	1.54 ± 0.05	2.04 ± 0.05
HP-WSOM	0.99 ± 0.06	1.67 ± 0.08	2.53 ± 0.08			

[a] Molar ratio.

[b] Mass ratio.